

Carbachol dimers with primary carbamate groups as homobivalent modulators of muscarinic receptors.

Rosanna Matucci,^a Cristina Bellucci,^b Maria Vittoria Martino,^b Marta Nesi,^a Dina Manetti,^b Jessica Welzel,^c Ulrike Bartz,^d Janine Holze,^c Christian Tränkle,^c Klaus Mohr,^c Angelica Mazzolari,^e Giulio Vistoli,^e Silvia Dei,^b Elisabetta Teodori,^b Maria Novella Romanelli^b

^aDepartment of Neuroscience, Psychology, Drug Research and Child's Health, Section of Pharmacology and Toxicology, University of Florence, Viale G. Pieraccini 6, 50139 Firenze, Italy.

^bDepartment of Neuroscience, Psychology, Drug Research and Child's Health, Section of Pharmaceutical and Nutraceutical Sciences, University of Florence, Via Ugo Schiff 6, 50019 Sesto Fiorentino, Italy.

^cDepartment of Pharmacology & Toxicology, Institute of Pharmacy, University of Bonn, Gerhard-Domagk-Str. 3, 53121 Bonn, Germany.

^dDepartment of Natural Sciences, H-BRS University of Applied Sciences, von-Liebig-Str. 20, 53359 Rheinbach, Germany.

^eDepartment of Pharmaceutical Sciences, University of Milan, Via Mangiagalli 25, 20133 Milano, Italy.

Corresponding author

Rosanna Matucci, Department of Neuroscience, Psychology, Drug Research and Child's Health, Section of Pharmacology and Toxicology, University of Florence, Viale G. Pieraccini 6, 50139 Firenze, Italy. Tel +39 055 2758280 e-mail: rosanna.matucci@unifi.it

Classification

Molecular and cellular pharmacology

Abstract

Although agonists and antagonists of muscarinic receptors have been known for long time, there is renewed interest in compounds (such as allosteric or bitopic ligands, or biased agonists) able to differently and selectively modulate these receptors. As a continuation of our previous research, we designed a new series of dimers of the well-known cholinergic agonist carbachol. The new compounds were tested on the five cloned human muscarinic receptors (hM₁₋₅) expressed in CHO cells by means of equilibrium binding experiments, showing a dependence of the binding affinity on the length and position of the linker connecting the two monomers. Kinetic binding studies revealed that some of the tested compounds were able to slow the rate of NMS dissociation, suggesting allosteric behavior, also supported by docking simulations. Assessment of ERK1/2 phosphorylation on hM₁, hM₂ and hM₃ activation showed that the new compounds are endowed with muscarinic antagonist properties. At hM₂ receptors, some compounds were able to stimulate GTP γ S binding but not cAMP accumulation, suggesting a biased behavior.

Keywords

Muscarinic acetylcholine receptor (mAChR), carbachol dimers, allosteric modulation

Chemical compounds studied in this article:

Carbachol chloride (PubChem CID: 5831); Acetylcholine chloride (PubChem CID: 6060); Hexamethonium chloride (PubChem CID: 93550); Gallamine triethiodide (PubChem CID: 6172); McN-A-343 chloride (PubChem CID: 5926); Atropine sulphate (PubChem CID: 64663).

1. Introduction

Five different muscarinic acetylcholine receptor (mAChR) subtypes are known (M_1 - M_5) which are widely distributed inside and outside the CNS and involved in many physiological processes. Muscarinic ligands are mainly used in clinical settings to treat chronic obstructive pulmonary disease, overactive bladder and Sjögren's syndrome, but selective agonists or antagonists of these proteins may be potentially useful in several other disorders or conditions (Kruse et al., 2014; Wess et al., 2007).

Muscarinic receptors can be modulated by means of ligands interacting with the orthosteric or allosteric site(s) whose topography has been determined from recent crystal structures of ligand-complexed M_1 - M_4 receptors (Haga et al., 2012; Kruse et al., 2012; Kruse et al., 2013; Thal et al., 2016). Modulation from an allosteric site is particularly attractive since these regions are much less conserved than the orthosteric one for the endogenous neurotransmitter; with allosteric ligands therefore it should be possible to achieve the subtype-selectivity which has been elusive with orthosteric modulators (Bock et al., 2018). The location of an allosteric site near the orthosteric one led to the design of dualsteric/bitopic ligands (i.e. compounds which can simultaneously bind to both sites) obtained by hybridizing non-selective orthosteric ligands with subtype-selective allosteric modulators. These bivalent ligands can display interesting properties, such as subtype selectivity, functional selectivity, and protean agonism (Bock et al., 2018; De Min et al., 2017; Schrage and Kostenis, 2017; Valant et al., 2012). A

muscarinic agonist, 4-[[[(3-chlorophenyl)carbamoyl]oxy]-N,N,N-trimethylbut-2-yn-1-ammonium chloride (McN-A-343) (Mitchelson, 2012), was recently recognized as a bitopic ligand (May et al., 2007; Valant et al., 2008). This compound showed about 10-fold higher activity on G₁₅-coupled M₂ receptors compared with G_i-coupled M₂ receptors, displaying functional selectivity. Some hybrids composed of the orthosteric agonist xanomeline and the allosteric agonist 1-[3-(4-butyl-1-piperidinyl)propyl]-3,4-dihydro-2(1H)-quinolinone (77-LH-28-1) showed different abilities to engage Gq or β -arrestin via M₁ mAChRs, compared to both lead compounds (Bonifazi et al., 2014). A recent paper proposed that the extent of closure of the extracellular allosteric binding site influences the intracellular coupling to distinct signaling pathways, suggesting a mechanistic explanation of biased agonism (Bermudez et al., 2017). However, stimulus bias has been displayed also by orthosteric muscarinic ligands (see refs Gregory et al., 2010 and Pronin et al., 2017 as examples).

In a previous paper we described a series of carbachol dimers (compounds **1a-f**, **2a-f**, Fig. 1); kinetic binding studies and docking simulations have suggested a bitopic behavior for some of them (Matucci et al., 2016). Compounds **1a-f** and **2a-f** are symmetric dimers in which the two monomers are connected through the carbamic nitrogen atoms by means of a methylene chain of variable length. In this paper we report the activity of their isomers, having the two agonist units linked by a polymethylene spacer connecting the cationic nitrogen atoms (compounds **3a-e** and **4a-e**, Fig. 1); tertiary amines and ammonium derivatives were both prepared. In addition, a hybrid compound has been synthesized (**5**) where a 10-methylene chain connects the carbamic nitrogen atom of one monomer with the basic nitrogen atom of the second one. To verify the importance of the presence of both agonist units, compound **6** and the synthetic intermediates **7d,e** were also tested. The activity of the compounds was measured in binding and functional studies on CHO cells expressing the five hM₁₋₅ receptors; docking methods

were used to rationalize the outcome of binding experiments. The results were compared to those found for the previously synthesized **1a-f** and **2a-f**.

FIG. 1 NEAR HERE

2. Materials and methods

2.1. Drugs

The following drugs were used: carbachol chloride, acetylcholine chloride, examethonium chloride, McN-A-343 chloride, gallamine triethiodide, atropine sulphate salt monohydrate and (-)-scopolamine methylbromide purchased from Sigma-Aldrich SRL, Milano, Italy; [³H]N-methylscopolamine chloride specific activity range 2,590–3,200 GBq/mmol and [³⁵S]guanosine-5'- γ -thiotriphosphate specific activity 46.25 TBq/mmol from Perkin-Elmer Life and Analytical Science, Monza, Milano, Italy. Pertussis toxin (PTX) was purchased from Biotrend (Cologne, Germany). All other reagents were purchased from Sigma-Aldrich SRL (Milano, Italy) unless stated otherwise. Compounds **3a-e**, **4a-e**, **5**, **6** and **7d-e** were prepared as reported in Appendix A.

2.2 Biological studies

Equilibrium radioligand binding assays, dissociation kinetic assays, guinea-pig ileum preparations, and the Extracellular Signal-Regulated Kinase (ERK1/2) Phosphorylation Assays were performed as previously described (Matucci et al., 2016). The organs used in this article derive from programs for sharing organs and tissues of animals sacrificed in the animal

house facility of the University of Florence, in compliance with the principle of reduction. The experiments described was approved from Institutional Animal Care and Use Committee (IACUC) of the University of Florence and from the Italian Ministry of Health (Authorization No. 54/2014-B), issued under the previous Italian Law Decree (No. 116/1992) on animal testing. With regard to data analysis for compounds **3a**, **3b** and **4a**, pIC_{0.5} values (i.e. the concentration at the inflection point of the respective inhibition curves) are reported instead of pK_i because these compounds did not completely displace [³H]NMS equilibrium binding at all muscarinic receptors subtypes studied, thus suggesting a non-competitive behavior. In all other cases, data from these experiments were fitted to a parametric function to derive best estimates of the IC₅₀ and slope factor; IC₅₀ values were then converted to binding constant K_i according to Cheng-Prusoff equation.

These parameters are presented as mean ± S.E.M. of at least three experiments, each one performed in duplicate, unless otherwise noted.

2.2.1 Data analysis:

Data generated from binding assays were analysed using Prism 5.02 (GraphPad Software Inc., San Diego, CA). Data points were fitted to models using nonlinear regression equations.

Some equations, regarding dissociation kinetic assays, were derived by Dr Nigel Birdsall and then formulated to be introduced into GraphPad Prism. According to the protocol developed by Lazareno and Birdsall (1995), one point kinetic data were analyzed as a function of time and then in order to obtain estimates of the affinity of an allosteric agent for the [³H]NMS-occupied receptor (K_{occ}) in a single step (equation 1).

$$k_{\text{off}}/(1+K_{\text{occ}} \times X) \quad (1)$$

k_{off} is the dissociation rate constant of the radioligand in the absence of X; X refers to the log

concentration of the allosteric ligand and $\log K_{\text{occ}}$ is its log affinity constant for the occupied receptor. This equation can also be used to directly estimate $\log K_{\text{occ}}$ by analyzing the amount of [^3H]NMS remaining at certain times at different concentrations of the allosteric modulators (see Lazareno and Birdsall, 1995).

2.3. GTP γ S binding assay

GTP γ S binding assay was performed as reported in previous papers (see ref Jäger et al., 2007). Curves were fitted with a “four parameter logistic function”; the respective curve slopes were not different from unity (F-test, $P > 0.05$).

2.4. cAMP-accumulation

Quantification of agonist-induced rise of intracellular cAMP was performed using CHO-hM₂ cells pretreated with 100 ng/ml⁻¹ PTX for 16-22 h, as described previously using a HTRF-cAMP dynamic kit (Cisbio, Bagnols-sur-Cèze, France) following the manufacturer’s instructions. cAMP content was detected dispensing 50,000 cells per well in a buffer containing Hanks’ balanced salt solution with 20 mM HEPES and 1 mM of the phosphodiesterase inhibitor IBMX. Fluorescence was quantified on a Mithras LB 940 multimode reader (Berthold Technologies, Bad Wildbad, Germany). Levels of cAMP were normalized to the amount of cAMP generated by 100 μM Acetylcholine (ACh).

2.5. Computational studies

With a view to investigating the molecular recognition of the proposed molecules, docking simulations were performed by applying the same computational protocols already reported in the previous study (Matucci et al., 2016), focusing attention on the hM₂ subtype. In detail, docking calculations involved the resolved structures in both active (PDB Id: 4MQT) and inactive (PDB Id: 3UON) conformations. The inactive structure was simulated retaining the co-crystallized QNB inhibitor in order to mimic the experimental conditions of the kinetic studies. Briefly, docking simulations were performed using PLANTS and focusing the search on a sphere large enough to encompass orthosteric and allosteric binding sites at the same time. For each ligand, 10 poses were generated using the ChemPLP scoring function and the obtained results were analyzed by ReScore+ (Vistoli et al., 2017).

3. Results

Compounds **3a-e** and **4a-e**, **5**, **6** and **7d-e** have been synthesized using standard methods (Appendix A). Derivatives **3a-e** and **4a-e** represent structural isomers of the previously described **1a-f** and **2a-f**, differing for the position of attachment of the polymethylene spacer; it was envisaged that with this new arrangement, the carbammic moiety could be free to establish the key contacts within the binding site, which appeared to be precluded for **1** and **2** (Matucci et al., 2016).

3.1. Equilibrium binding affinity

The affinity of compounds **3a-e**, **4a-e**, **5**, **6** and **7d-e** for the five human muscarinic receptor subtypes (hM₁-hM₅), measured in equilibrium binding experiments, is reported in Table 1 as pK_i or pIC_{0.5} and illustrated in Fig. S1 carbachol (CCh) and McN-A-343 have been taken as reference compounds.

TABLE 1 NEAR HERE

All the compounds were able to displace the radioligand [³H]NMS binding at all muscarinic receptor subtypes, in a concentration-dependent way and with different inhibitory propensity. Symmetric dimers **3c-e** and **4b-e** completely displaced specific radioligand binding at all receptor subtypes, while **3a,b** and **4a** did not, even at millimolar concentrations, giving pIC_{0.5} values <4 at some receptor subtypes (hM₂, hM₄ and hM₅ for **3a**, hM₃, hM₄ and hM₅ for **4a**, hM₄ for **3b**). When n ≥ 7, structural dimerization generally improved binding affinity with respect to carbachol, with the exception of compound **3c** on hM₂; among the shorter derivatives, **4b** (n = 5) showed pK_i values higher than carbachol only on hM₁ and hM₃. The affinity of bases **3a-e** regularly increased with increasing the length of the chain in all receptor subtypes (Fig. S1A). In contrast, for methiodides **4a-e** (Fig. S1B), in some cases the increment brought by two methylene units was small or absent. This was the case for **4c-4d** (n = 7 and 9, respectively) at hM₄ and hM₅, while at hM₃ affinity was slightly decreased. Nevertheless, **4e** (n = 11) was the most potent compound at each subtype, being equipotent with **4d** on the hM₂ receptor.

Contrary to what happened in the previously synthesized **1** and **2** series, where methiodides had higher affinity measures than the corresponding bases, for compounds **3** and **4** a permanent positive charge increased affinity only for a spacer length of n=7: affinity measures of **4c** were higher than those of **3c** at all subtypes. For compounds with n= 3, 5, 9 and 11 the affinity measures of bases were equal or higher than those of methiodides, apart from those cases when affinity measures were <4.

In general, symmetric dimers **3a-e** and **4a-e** did not show subtype selectivity of binding; only for the longer compounds (**3d-e**, **4d-e**, n = 9, 11) was the difference in affinity measures on

some subtypes higher than one order of magnitude. With the exclusion of compounds **3a-b** and **4a**, whose affinity measures could not be calculated for all receptor subtypes, symmetric dimer compounds showed the lowest apparent affinity measure at hM₃ and hM₅ receptors (Table 1, Fig. S1A,B).

The contribution to affinity of the second carbamate moiety was investigated by testing compounds **6**, **7d** and **7e**. N-undecyl derivative **6** showed similar binding constants at all subtypes (pK_i values ranging from 5.82±0.08 on hM₅ to 6.26±0.04 on hM₁), with pK_i values intermediate between those of **3c** and **3d**. With respect to **6**, compounds **7d** and **7e** possessed an additional basic moiety, which did not improve affinity but was actually detrimental for it at hM₃. With respect to bis-carbamate **3d**, monocarbamate **7d** showed lower affinity on hM₁ and hM₂ but not on hM₃ and hM₅, while the affinity of **7e** was much lower than that of **3e** on all subtypes (Table 1, Fig. S1C). This behavior suggested that the second carbachol unit gave an important contribution to the interaction of the long derivative **3e** (n=11) with all subtypes, while for **3d** (n = 9) its role was less important and limited to the hM₁ and hM₂ subtypes.

The hybrid compound **5**, carrying a 10-methylene chain as a linker, showed similar binding constants at all subtypes (pK_i values ranging from 6.33 at hM₂ to 6.90 at hM₁) (Table 1, Fig. S1C). Compared to the homodimers having similar linker's length, the pK_i values of **5** were intermediate between those of **3d** (n=9) and **3e** (n=11) at hM₁ and hM₄ but not at hM₂, hM₃ and hM₅; with respect to the previously described **1d** (n=9, pK_i in the range 6.53-7.89) and **1e** (n=11, pK_i in the range 6.29-7.16), the binding measure of **5** was lower. Compound **5** showed the lowest pK_i value on hM₂, its profile resembling that of compounds **1-2** (Matucci et al., 2016) and not that of **3-4**; the latter showed the lowest affinity measures at hM₃ and hM₅ receptors.

3.2. Kinetic binding studies

In order to detect a possible interaction with an allosteric site, the ability of selected compounds to affect the [³H]NMS dissociation rate was evaluated, using a one-point kinetic protocol as previously reported (Matucci et al., 2016; Lazareno and Birdsall, 1995); gallamine and McN-A-343 were taken as reference molecules. Representative graphs are shown in Fig. 2 for **3e** and gallamine.

FIG. 2 NEAR HERE

Panels A-B show the increase of the specifically M₂ receptor-bound [³H]NMS, due to the reduction of its dissociation rate by the ligand studied, as a function of time with increasing concentrations of the modulators. In Fig. 2D the increase of [³H]NMS bound to the receptor is shown as a function of increasing concentrations of allosteric modulators. The top data point (shown at log [agent] = -1) represents [³H]NMS binding before dissociation starts. The curves extrapolate to this value, implying that these compounds could substantially slow down [³H]NMS dissociation at a sufficiently high concentration. Like gallamine, **3e**, taken as an example, markedly inhibited the dissociation of [³H]NMS from hM₂ receptors, giving rise to an increase in residual [³H]NMS binding at the time point selected (t= 20 min), with the curve being well defined. Analysis of the kinetic data in Fig. 2A-B, according to Lazareno and Birdsall (Lazareno and Birdsall, 1995), gave logK_{occ} values which represent the binding affinity at the NMS-occupied receptor and are reported in Table 2 and in Fig.S2.

TABLE 2 NEAR HERE

As expected, gallamine showed preference for the NMS-occupied hM₂ subtype (Table 2). All tested compounds were able to slow the [³H]NMS dissociation rate, but with different potency depending on their structure and the receptor subtype.

The change in activity of compounds **3a-e** with respect to the linker length (Table 2, Fig. S2A) was similar on all subtypes, **3c** being the least active compound (n = 7) and **3d** (n = 9) the most active. Methiodides **4a-e** (Table 2, Fig. S2B) showed a similar trend on hM₁, on which the logK_{occ} values for **4d** and **4e** were similar. On the contrary, at hM₂ receptors the apparent allosteric affinity of methiodides **4a-e** regularly increased with chain length, while at the other subtypes the trend was different and uneven. The longest compound **4e** (n = 11) was the most active quaternary derivative on all subtypes except hM₃ and hM₅.

A permanent positive charge had no clear-cut effect on radioligand dissociation: for short compounds **3a,b** and **4a,b** (n = 3, 5) the difference in logK_{occ} values between bases and quaternary compounds was very small. A difference greater than 0.5 log unit could be seen for **3c-4c** (n = 7), at all subtypes except hM₁, and for **3e-4e** (n = 11) only on hM₁; at these subtypes, methiodides **4c** and **4e** were more potent than the corresponding bases **3c** and **3e**. Base **3d** (n = 9) was more potent than its quaternary ammonium derivative **4d** on all subtypes. As a general trend, the logK_{occ} values of longer derivatives **3c-e** and **4c-e** (n = 9-11) for the occupied receptor were lower at hM₃ and hM₅ compared to the other receptor subtypes. This affinity profile was found also for the previously described series **1** and **2**, and it was shared also by hybrid **5** and amines **7d,e** (Table 2). Among the tested compounds, **3d** appeared to be the most potent one on all the receptor subtypes.

When n = 9, the presence of both carbamate groups increased the retarding action via the allosteric site: logK_{occ} estimates for compound **3d** were higher than those of **6** and **7d** at all receptor subtypes, with large differences at hM₂ and hM₄ and, with respect to **6**, also at hM₁.

When n = 11 (compound **3e**), the contribution of the second carbamate moiety was significant

with respect to **6** only at hM₁ and hM₂, as it increased the affinity measure 8.5 and 11 times, respectively. With respect to **7e**, the second carbamate moiety did not affect activity significantly, but at hM₁ receptors it was actually detrimental, since affinity of **3e** was 3-fold lower than that of **7e**.

3.3. Functional studies on isolated guinea pig ileum

As done for the previous series (Matucci, 2016), the new compounds were tested for their functional activity on guinea pig ileum, tissue in which M₃ than M₂ receptor sites are mainly present (Barocelli et al., 1993). All compounds, with the exception of **3e** and **5**, were able to evoke weak smooth muscle contractions (data not shown) which, however, were not antagonized by 1 nM atropine (which is able to antagonize the contractions induced by ACh and CCh), nor by the nicotinic antagonist hexamethonium (30 μM). This behavior could imply the involvement of a receptor system different from the cholinergic one, which was not further investigated. Compounds **5**, **6**, **7d** and **7e** behaved as weak antagonists (pK_B <5), being able to reduce contractions induced by ACh. Compound **3e** was devoid of activity both as agonist and antagonist, despite the micromolar affinity displayed in equilibrium binding studies (cf. Table 1) and a measurable binding propensity to NMS-occupied hM₁₋₅ receptors as quantified by logK_{occ} (cf. Table 2).

3.4. ERK 1/2 phosphorylation

To determine the functional activity of the compounds on muscarinic receptors, selected molecules (**3d-e**, **4d-e**, **7d-e**) were evaluated in ERK 1/2 phosphorylation assays in CHO cells stably expressing hM₁, hM₂ and hM₃ receptor subtypes. When tested alone up to a 100 μM

concentration, none of the compounds displayed agonistic activity (data not shown). Thus, their antagonistic properties against 10 nM ACh were assessed. The results, reported in Fig. 3A-C, show that a 100 μ M concentration of the compounds was able to reduce ACh-induced ERK 1/2 phosphorylation to different extents depending on the receptor subtype. At the hM₁ receptor (Fig. 3A) all tested compounds behaved as antagonists with the exception of **7d**, which was devoid of activity. At the hM₂ receptor (Fig. 3B) compounds **3d** and **4e** effectively reduced ACh stimulation, while the antagonistic effect of **4d**, **3e**, **7d** and **7e** was weaker or absent. At the hM₃ receptor (Fig. 3C) all tested compounds displayed an antagonistic effect, which was strong for **3d**, **4e**, **7d** and **7e** and much weaker, but still significant, for **4d** and **3e**. These results highlight for some compounds a certain degree of selectivity: for instance, **7d** was able to strongly antagonize ACh-induced ERK phosphorylation at hM₃ but it was ineffective at hM₁ and hM₂ receptors.

FIG. 3 NEAR HERE

3.5. Interaction with G proteins via hM₂ receptors

Activation of hM₂ muscarinic receptors was measured by means of [³⁵S]GTP γ S binding assays, performed according to previously reported protocols (Jäger et al., 2007). Initial pilot experiments had shown that specific [³H]NMS hM₂ equilibrium binding as defined by 10 μ M atropine to define nonspecific binding was concentration-dependently displaced by the test-compounds 4b-4e to 0% specific binding revealing the hM₂ receptor to be a target structure for them (data not shown).

Dose response curves for agonist mediated receptor activation are reported in Fig. 4; statistical parameters obtained from curves fitted to the mean data values are summarised in Table S1.

FIG. 4 NEAR HERE

Contrary to what happened in ERK assays, in this system test compounds **4b-e** produced receptor activation, being able to stimulate [³⁵S]GTPγS binding, albeit with low intrinsic activity. Their maximal effect was about 20 % of the maximum [³⁵S]GTPγS binding produced by the full agonists carbachol (100 μM) and acetylcholine (100 μM), thus behaving as weak partial agonists.

To further investigate functional activity, selected compounds (**4b-e**) were evaluated in a cAMP-accumulation assay applying CHO cells stably expressing the human M₂-receptor (hM₂). In contrast, none of the tested compounds (**4b-e**) at any concentration was able to induce a cAMP-accumulation significantly different from baseline on this G_s-signaling pathway (data not shown). In comparison to the results of the GTPγS binding experiments, compounds **4b-e** exhibited a G_i over G_s signaling bias compared with ACh and CCh.

3.7. Docking studies

As anticipated under Methods, docking simulations were focused on the hM₂ receptor by comparing its active and inactive conformations. When comparing the here obtained docking poses within the active hM₂ conformation with those already published (Matucci et al., 2016), one might notice a similar effect of the linker length on the observed binding modes. Indeed, the short derivatives (n < 7) cannot simultaneously occupy both orthosteric and allosteric

binding sites and tend to be completely accommodated within the orthosteric binding site, while the molecules with longer chains appeared to be able to engage both binding sites.

Unlike the previously reported dimers **1** and **2**, where the carbachol unit within the orthosteric site was always unable to elicit the same key interactions stabilized by the carbachol ligand alone [18], compounds **3** and **4** were almost always able to optimize their contacts within the orthosteric site.

In more detail, the ligands endowed with short linkers can assume three possible binding modes since they are accommodated within the orthosteric site, within the allosteric pocket or in-between. Thus, the computed poses for the shortest derivatives (**3a** and **4a**, $n = 3$) are roughly equally distributed between orthosteric and allosteric binding site even though the poses within the orthosteric pocket always represent the top scores. The intermediate poses represent an energy disfavored minority. Also the derivatives with $n = 5$ (**3b** and **4b**) show similar distributions with the best poses within the orthosteric site (as displayed in Fig. 5A) even though the intermediate poses progressively increase their relevance and indeed the ligands with $n = 7$ (**3c** and **4c**) preferentially assume in-between poses by which they properly occupies both binding pockets. Similar distributions are observed for longer derivatives even though all these longer compounds show some poses in which they are accommodated within the allosteric pocket only. Collectively, one may notice that the short ligands are able to occupy the allosteric site only in a less than half of the computed complexes which never correspond to best solution, while the longer derivatives are always able to be inserted within the allosteric cavity.

To exemplify the above described trends, Fig. 5 compares the best putative complexes as generated for ligands endowed with short (**3b**, $n = 5$, Fig. 5A) and long (**3d**, $n = 9$, Fig. 5B) linker and confirms that in both complexes at least one carbachol unit was properly

accommodated within the orthosteric site, while only the **3d** is able to insert the second unit within the allosteric pocket.

FIG. 5 NEAR HERE

The above discussed results are in agreement with the docking simulations based on the inactive hM₂ structure in complex with the co-crystallized quinuclidyl benzylate (QNB) inhibitor, where only the long derivatives were able to afford satisfactory complexes while showing more superficial poses compared to the corresponding compounds of set **1** and **2**. For example, Fig. 5C shows the putative complex as computed for **3d** which exhibits the highest log K_{occ} value. Both carbachol units are able to contact Glu175 and differ for the arrangement of carbamate functions since one carbamate remains in a superficial region while the second function approach the orthosteric cavity. Notably, a carbachol unit shows within the allosteric cavity a pose very similar to that already seen in the active hM₂ structure, thus suggesting that the arrangement of the orthosteric site does not markedly affect the accessibility of the allosteric cavity. The short derivatives are seen to approach the orthosteric cavity where they unsuitably interfere with the key residues of the orthosteric binding site thus competing with the QNB binding. The reported affinity and kinetic data confirm that the involvement of this empty space around the orthosteric pocket has an overall detrimental role when preventing the correct accommodation of the orthosteric ligands.

Altogether, the comparison of docking results for the two sets of carbachol dimers suggests that compounds **3** and **4** are more capable than compounds **1** and **2** to occupy the orthosteric binding site, a trend which can be ascribed to the different arrangement of the two key interacting moieties (i.e. the ammonium head and the carbamate function) which only in **3** and **4** parallels the corresponding arrangement of the hM₂ interacting residues. In contrast

compounds **3** and **4** are less capable than compounds **1** and **2** to occupy the allosteric binding site and this can be explained by considering the greater distance between the ammonium heads in the first set, having the carbachol units linked through their carbamate moieties, compared to the new dimers.

4. Discussion

This paper reports the characterization of a new series of carbachol dimers (compounds **3a-e** and **4a-e**) in which the two monomers are connected through the choline nitrogen atoms. The new compounds share some features with the previously characterized series **1a-f** and **2a-f**: a lack of selectivity toward one of the five muscarinic receptors, and a progressive increase of affinity by elongating the linker's chain, observed in equilibrium binding studies (Fig. S1, Table 1). However, some differences are also evident: in the new series, quaternarization of the amine moiety did not generally increase affinity, with the exception of compounds with $n = 7$, as pK_i values for **4c** are higher than those of **3c** on all subtypes. In addition, while compounds belonging to the **1** and **2** series show higher affinity at hM_3 and hM_5 (Matucci et al., 2016), compounds **3a-e** and **4a-e** show the lowest apparent affinity on these subtypes. Docking studies also highlight some differences. In fact, for compounds **3** and **4** one carbachol unit in the orthosteric site is able to elicit the key interactions engaged by the carbachol ligand alone (i.e ion-pairing with Asp103 and H-bonds) with a correct geometry, even when the linker is long enough to allow for a bitopic binding.

Kinetic binding studies also show a different behavior between series of compounds. In fact, in the old series (**1**, **2**) affinity for the allosteric site in NMS-occupied hM receptors increased smoothly with the linker's elongation, with the only exception of the compound with a six-methylene chain (**1f**, **2f**); the effect was more evident for the tertiary amines **1a-e** compared to

the quaternary ammonium analogs **2a-e**. On the contrary, the increase of $\log K_{occ}$ values for amines **3a-e** is not constant (Table 2, Fig. S2A): the jump going from $n=7$ (**3d**) to $n=9$ (**3e**) is associated to an increase of apparent affinity of about two orders of magnitude on hM₁, hM₂ and hM₄ mAChRs, and about one on the hM₃ and hM₅ subtypes. A similar trend is observed for methiodides **4a-e** only on hM₁ mAChR. This behavior is consistent with a change in the binding mode of the compounds, allowing a much better fit within the receptor binding pocket, at the allosteric site, since the orthosteric one is occupied by NMS.

Functional experiments gave contradicting results. On guinea-pig ileum the compounds behaved as much weaker agonist with respect to carbachol; however, the evoked contractions were not antagonized by atropine, nor by hexamethonium. This finding suggests that they do not depend on the cholinergic transmission; however, an activation of muscarinic receptors not blocked by muscarinic antagonist (QNB) was reported some years ago by Jakubik et al (Jakubík et al., 1996). Similarly to compounds **1c-e**, new compounds **5**, **6**, **7d** and **7e**, behaved as antagonists, although with lower potency.

Applying the ERK1/2 phosphorylation assay, performed at hM₁, hM₂ and hM₃ AChRs in CHO cells, selected compounds (**3d-e**, **4d-e**, **7d-e**) showed only antagonist properties, being able to reduce the effect elicited by ACh (Fig. 5). On the contrary, at hM₂ receptors methiodides **4b-e** stimulated GTP γ S binding with a maximum effect of roughly 20% with respect to the E_{max} evoked by CCh, demonstrating a partial agonist effect. This suggests that structural dimerization of the compounds did not completely abolish an agonistic effect, at least not at the hM₂ subtype, although the intrinsic activity was low. However, differently from carbachol, these compounds were able to initiate hM₂ receptor coupling only with G_i, but not with G_s proteins. Since ERK1/2 phosphorylation is believed to be an example of arrestin-dependent signaling in GPCR (Rajagopal et al., 2010), these results seem to suggest for methiodides **4b-e** at hM₂ receptors a biased activity toward G_i in comparison to the G_s and

β -arrestin pathways. Although binding studies did not highlight subtype selectivity, some compounds showed a different activity on the three muscarinic receptors tested (hM₁, hM₂ and hM₃) suggesting some degree of functional selectivity.

In conclusion, we have prepared a new series of homodimers of the well-known cholinergic agonist carbachol. The compounds have been analyzed by means of equilibrium and kinetic binding studies; docking simulations on hM₂ receptor supported the view that some compounds may bind in a bitopic fashion. Functional experiments showed that homodimerization, connecting two carbachol units through the choline nitrogen atoms, gave derivatives which maintained some agonistic activity, being able to stimulate the binding of GTP γ S to the Gi protein. The inability to couple with Gs, or to stimulate ERK1/2 phosphorylation suggests some degree of functional pathway selectivity for these molecules. A more in-depth investigation on the ligand bias potential of these compounds is underway and will be reported in due time.

5. Acknowledgments

This work was supported by grants from MIUR – Italy (PRIN 2009, 2009ESXPT2_002).

6. Appendix A:

Supplementary Data. Synthetic procedures and the physicochemical properties of the compounds synthesized in this study.

7. References

Barocelli, E., Chiavarini, M., Ballabeni, V., Bordi, F., Impicciatore, M., 1993. Interaction of selective compounds with muscarinic receptors at dispersed intestinal smooth muscle cells. *Br. J. Pharmacol.* 108, 393-397.

Bermudez, M., Bock, A., Krebs, F., Holzgrabe, U., Mohr, K., Lohse, M.J., Wolber, G., 2017. Ligand-Specific Restriction of Extracellular Conformational Dynamics Constrains Signaling of the M2 Muscarinic Receptor. *ACS Chem. Biol.* 12, 1743-1748.

Bock, A., Schrage, R., Mohr, K., 2018. Allosteric modulators targeting CNS muscarinic receptors. *Neuropharmacology* 136, 427-437.

Bonifazi, A., Yano, H., Del Bello, F., Farande, A., Quaglia, W., Petrelli, R., Matucci, R., Nesi, M., Vistoli, G., Ferré, S., Piergentili, A., 2014. Synthesis and Biological Evaluation of a Novel Series of Heterobivalent Muscarinic Ligands Based on Xanomeline and 1-[3-(4-Butylpiperidin-1-yl)propyl]-1,2,3,4-tetrahydroquinolin-2-one (77-LH-28-1). *J. Med. Chem.* 57, 9065-9077.

De Min, A., Matera, C., Bock, A., Holze, J., Kloeckner, J., Muth, M., Traenkle, C., De Amici, M., Kenakin, T., Holzgrabe, U., Dallanoce, C., Kostenis, E., Mohr, K., Schrage, R., 2017. A new molecular mechanism to engineer protean agonism at a G protein-coupled receptor. *Mol. Pharmacol.* 91, 348-356.

Gregory, K.J., Hall, N.E., Tobin, A.B., Sexton, P.M., Christopoulos, A., 2010. Identification of Orthosteric and Allosteric Site Mutations in M2 Muscarinic Acetylcholine Receptors That Contribute to Ligand-selective Signaling Bias. *J. Biol. Chem.* 285, 7459-7474.

Haga, K., Kruse, A.C., Asada, H., Yurugi-Kobayashi, T., Shiroishi, M., Zhang, C., Weis, W.I., Okada, T., Kobilka, B.K., Haga, T., Kobayashi, T., 2012. Structure of the human M2 muscarinic acetylcholine receptor bound to an antagonist. *Nature* 482, 547.

Jäger D., Schmalenbach C., Prilla S., Schrobang J., Kebig A., Sennwitz M., Heller E., Tränkle C., Holzgrabe U., Höltje H.D., Mohr K. 2007. Allosteric small molecules unveil a role of an

extracellular E2/transmembrane helix 7 junction for G protein-coupled receptor activation. *J. Biol. Chem.* 282, 34968-34976.

Jakubík, J., Bacáková, L., Lisá, V., el-Fakahany, E.E., Tucek, S., 1996. Activation of muscarinic acetylcholine receptors via their allosteric binding sites. *PNAS* 93, 8705-8709.

Kruse, A.C., Hu, J., Pan, A.C., Arlow, D.H., Rosenbaum, D.M., Rosemond, E., Green, H.F., Liu, T., Chae, P.S., Dror, R.O., Shaw, D.E., Weis, W.I., Wess, J., Kobilka, B.K., 2012. Structure and dynamics of the M3 muscarinic acetylcholine receptor. *Nature* 482, 552.

Kruse, A.C., Kobilka, B.K., Gautam, D., Sexton, P.M., Christopoulos, A., Wess, J., 2014. Muscarinic acetylcholine receptors: novel opportunities for drug development. *Nat. Rev. Drug. Discov.* 13, 549-560.

Kruse, A.C., Ring, A.M., Manglik, A., Hu, J., Hu, K., Eitel, K., Hubner, H., Pardon, E., Valant, C., Sexton, P.M., Christopoulos, A., Felder, C.C., Gmeiner, P., Steyaert, J., Weis, W.I., Garcia, K.C., Wess, J., Kobilka, B.K., 2013. Activation and allosteric modulation of a muscarinic acetylcholine receptor. *Nature* 504, 101-106.

Lazareno, S., Birdsall N.J., 1995. Detection, quantitation, and verification of allosteric interactions of agents with labeled and unlabeled ligands at G protein-coupled receptors: interactions of strychnine and acetylcholine at muscarinic receptors. *Mol. Pharmacol.* 48, 362-378.

Matucci, R., Nesi, M., Martino, M.V., Bellucci, C., Manetti, D., Ciuti, E., Mazzolari, A., Dei, S., Guandalini, L., Teodori, E., Vistoli, G., Romanelli, M.N., 2016. Carbachol dimers as homobivalent modulators of muscarinic receptors. *Biochem. Pharmacol.* 108, 90-101.

May, L.T., Avlani, V.A., Langmead, C.J., Herdon, H.J., Wood, M.D., Sexton, P.M., Christopoulos, A., 2007. Structure-Function Studies of Allosteric Agonism at M2 Muscarinic Acetylcholine Receptors. *Mol. Pharmacol.* 72, 463-476.

Mitchelson, F.J., 2012. The pharmacology of McN-A-343. *Pharmacol. Ther.* 135, 216-245.

Pronin, A.N., Wang, Q., Slepak, V.Z., 2017. Teaching an Old Drug New Tricks: Agonism, Antagonism, and Biased Signaling of Pilocarpine through M3 Muscarinic Acetylcholine Receptor. *Mol. Pharmacol.* 92, 601-612.

Rajagopal, S., Rajagopal, K., Lefkowitz, R.J., 2010. Teaching old receptors new tricks: biasing seven-transmembrane receptors. *Nat. Rev. Drug. Discov.* 9, 373.

Schrage, R., Kostenis, E., 2017. Functional selectivity and dualsteric/bitopic GPCR targeting. *Curr. Opin. Pharmacol.* 32, 85-90.

Thal, D.M., Sun, B., Feng, D., Nawaratne, V., Leach, K., Felder, C.C., Bures, M.G., Evans, D.A., Weis, W.I., Bachhawat, P., Kobilka, T.S., Sexton, P.M., Kobilka, B.K., Christopoulos, A., 2016. Crystal structures of the M1 and M4 muscarinic acetylcholine receptors. *Nature* 531, 335.

Valant, C., Gregory, K.J., Hall, N.E., Scammells, P.J., Lew, M.J., Sexton, P.M., Christopoulos, A., 2008. A Novel Mechanism of G Protein-coupled Receptor Functional Selectivity: Muscarinic partial agonist McN-A-343 as a bitopic orthosteric/allosteric ligand. *J. Biol. Chem.* 283, 29312-29321.

Valant, C., Robert Lane, J., Sexton, P.M., Christopoulos, A., 2012. The Best of Both Worlds? Bitopic Orthosteric/Allosteric Ligands of G Protein–Coupled Receptors. *Annu. Rev. Pharmacol.* 52, 153-178.

Vistoli, G., Mazzolari, A., Testa, B., Pedretti, A., 2017. Binding Space Concept: A New Approach To Enhance the Reliability of Docking Scores and Its Application to Predicting Butyrylcholinesterase Hydrolytic Activity. *J. Chem. Inf. Model.* 57, 1691-1702.

Wess, J., Eglen, R.M., Gautam, D., 2007. Muscarinic acetylcholine receptors: mutant mice provide new insights for drug development. *Nat. Rev. Drug Discov.* 6, 721-733.

Legends to Fig.s

Fig. 1. Structure of the reference molecules and newly synthesized compounds.

Fig. 2. Representative graphs for one-point kinetic assay. Panels A-D show the course of [³H]NMS dissociation from the hM₂ receptor in the presence of increasing concentrations of the selected ligands **3e** (A) and gallamine (B) added in combination with atropine (10 μM) as a function of time. The incubation time point selected in each case was 20 min, around 2-3 times the k_{off} of [³H]NMS at hM₂ receptors. Please notice that the control curve (black) in panel A lays below the green curve. Panel D: representative curves of residual specific binding obtained by transposing the respective binding levels from one-point kinetic assays for **3e** and gallamine at [³H]NMS-occupied M₂ receptors to illustrate the promoting effect of allosteric retardation on specific [³H]NMS receptor binding by a four parameter logistic curve fitting. The data point at log [agent] = -1 represents the [³H]NMS bound in the absence of added atropine (10 μM) and “allosteric” ligand.

Fig. 3. Determination of ERK1/2 phosphorylation in intact cells stably transfected with (A) hM₁, (B) hM₂ and (C) hM₃ receptors. Concentrations used were the following: acetylcholine (10 nM), tested compounds (100 μM) and atropine (10 μM). Data are illustrated as a percentage of the response mediated by 10% serum and are presented as mean ± S.E.M. of three to four experiments, each one performed in quadruplicate. Parameters were statistically evaluated with one-way ANOVA followed by Tukey’s Multiple Comparison Test (vs. ACh as the control). *** P<0.0001; ** P<0.001; *P<0.05.

Fig. 4. Stimulation of M-receptor mediated [³⁵S]GTPγS binding by compounds **4b-e** in CHO-hM₂ membranes, in comparison to ACh and CCh. [³⁵S]GTPγS binding in CHO-hM₂ membranes is plotted versus increasing (log)-concentrations of the respective ligands

(abscissa). E_{\max} values are expressed as a percentage of the maximal [^{35}S]GTP γ S binding induced by CCh being 100%. Experiments were performed with a final protein concentration of 40 $\mu\text{g ml}^{-1}$ and a [^{35}S]GTP γ S concentration of 0.07 nM. Incubation took place at 30 °C for one hour. Data are means \pm S.E.M. from three to eight independent experiments performed in quadruplicate or triplicate. Error bars are only visible when exceeding the symbols. Curves were fitted with a “four parameter logistic function” and the curve slope not different from unity (F-test, $P > 0.05$). Numerical estimates of selected parameters obtained from the curve analyses are listed in Table S1.

Fig. 5. Main interactions stabilizing the putative complexes for **3b** (A) and **3d** (B) within the active hM₂ structure as well as for **3d** (C) within the inactive hM₂ structure in complex with QNB (depicted in yellow).

Table 1. Parameters describing estimated equilibrium binding affinity of the tested compounds (see structures shown in fig.1) for human cloned muscarinic receptors expressed in CHO-K1 cells membranes. Results are expressed as inhibition binding constants, pK_i , or as $pIC_{0.5}$ (in round brackets), when the compound did not fully displace the radioligand. Values are reported as means of 3-4 experiments \pm S.E.M.

Compound	n	X	hM ₁	hM ₂	hM ₃	hM ₄	hM ₅
3a	3	NMe	(4.30 \pm 0.16)	(<4)	(4.02 \pm 0.16)	(<4)	(<4)
4a	3	NMe ₂	(4.37 \pm 0.06)	(4.69 \pm 0.07)	(<4)	(<4)	(<4)
3b	5	NMe	(4.46 \pm 0.06)	(5.07 \pm 0.04)	(4.05 \pm 0.20)	(<4)	(4.00 \pm 0.11)
4b	5	NMe ₂	4.97 \pm 0.06	5.00 \pm 0.06	4.68 \pm 0.07	5.18 \pm 0.07	4.16 \pm 0.08
3c	7	NMe	5.53 \pm 0.03	5.64 \pm 0.05	5.09 \pm 0.05	5.48 \pm 0.09	4.80 \pm 0.04
4c	7	NMe ₂	5.99 \pm 0.03	6.13 \pm 0.06	5.41 \pm 0.03	5.80 \pm 0.03	5.11 \pm 0.04
3d	9	NMe	6.73 \pm 0.04	6.68 \pm 0.06	5.50 \pm 0.03	6.16 \pm 0.04	5.33 \pm 0.03
4d	9	NMe ₂	6.28 \pm 0.03	6.75 \pm 0.08	5.18 \pm 0.05	5.74 \pm 0.05	5.08 \pm 0.04
3e	1	NMe	7.42 \pm 0.06	7.45 \pm 0.06	6.45 \pm 0.04	7.15 \pm 0.06	6.32 \pm 0.04
4e	1	NMe ₂	6.95 \pm 0.04	6.82 \pm 0.06	6.12 \pm 0.03	6.38 \pm 0.04	5.80 \pm 0.04
5	-	-	6.90 \pm 0.06	6.33 \pm 0.07	6.54 \pm 0.10	6.66 \pm 0.10	6.43 \pm 0.13
6	-	-	6.26 \pm 0.04	6.00 \pm 0.04	6.25 \pm 0.07	6.07 \pm 0.05	5.82 \pm 0.08
7d	9	-	6.31 \pm 0.01	6.30 \pm 0.03	5.75 \pm 0.09	6.08 \pm 0.07	6.00 \pm 0.01
7e	1	-	6.47 \pm 0.21	6.16 \pm 0.06	5.46 \pm 0.07	5.90 \pm 0.06	5.75 \pm 0.01
Carbachol	-	-	4.42 \pm 0.10	5.92 \pm 0.07	4.36 \pm 0.10	5.20 \pm 0.07	4.16 \pm 0.09

Table 2. Log affinity estimates ($\log K_{occ}$) of the tested compounds (see structures shown in fig.1) at the indicated [^3H]NMS-occupied muscarinic receptor subtypes calculated as described in ref.18. Values are reported as means \pm S.E.M. of at least three experiments performed in duplicate.

Compound	n	X	hM ₁	hM ₂	hM ₃	hM ₄	hM ₅
3a	3	NMe	3.77 \pm 0.04	3.27 \pm 0.16	3.65 \pm 0.04	3.92 \pm 0.02	3.51 \pm 0.09
4a	3	NMe ₂ I	3.89 \pm 0.13	3.06 \pm 0.20	3.79 \pm 0.01	3.67 \pm 0.26	3.68 \pm 0.01
3b	5	NMe	3.59 \pm 0.17	3.48 \pm 0.20	3.48 \pm 0.20	3.72 \pm 0.07	3.40 \pm 0.15
4b	5	NMe ₂ I	3.64 \pm 0.11	3.42 \pm 0.11	3.96 \pm 0.01	3.90 \pm 0.04	3.85 \pm 0.04
3c	7	NMe	3.37 \pm 0.52	3.37 \pm 0.14	2.96 \pm 0.13	3.52 \pm 0.22	3.24 \pm 0.05
4c	7	NMe ₂ I	3.57 \pm 0.01	4.17 \pm 0.01	3.56 \pm 0.01	4.20 \pm 0.01	3.92 \pm 0.01
3d	9	NMe	5.32 \pm 0.14	5.79 \pm 0.12	4.14 \pm 0.23	5.36 \pm 0.12	4.16 \pm 0.07
4d	9	NMe ₂ I	4.73 \pm 0.12	4.65 \pm 0.06	4.09 \pm 0.08	3.84 \pm 0.09	3.70 \pm 0.15
3e	11	NMe	4.28 \pm 0.18	4.96 \pm 0.07	4.15 \pm 0.08	4.79 \pm 0.06	4.15 \pm 0.06
4e	11	NMe ₂ I	4.91 \pm 0.07	5.18 \pm 0.05	3.82 \pm 0.08	4.67 \pm 0.04	4.07 \pm 0.10
5	-	.	5.02 \pm 0.07	5.30 \pm 0.07	3.80 \pm 0.10	4.81 \pm 0.07	3.72 \pm 0.09
6	-	-	3.35 \pm 0.30	3.91 \pm 0.15	3.93 \pm 0.07	4.42 \pm 0.12	4.03 \pm 0.07
7d	9	-	4.98 \pm 0.13	4.57 \pm 0.08	4.01 \pm 0.04	4.36 \pm 0.06	3.87 \pm 0.12
7e	11	-	4.80 \pm 0.15	4.51 \pm 0.26	4.23 \pm 0.06	4.52 \pm 0.10	4.26 \pm 0.06
Gallamine	-	-	4.15 \pm 0.03	5.16 \pm 0.07	4.20 \pm 0.05	4.56 \pm 0.08	4.30 \pm 0.07
McN-A-343			3.57 \pm 0.26	3.39 \pm 0.15	3.42 \pm 0.16	3.64 \pm 0.15	3.68 \pm 0.15

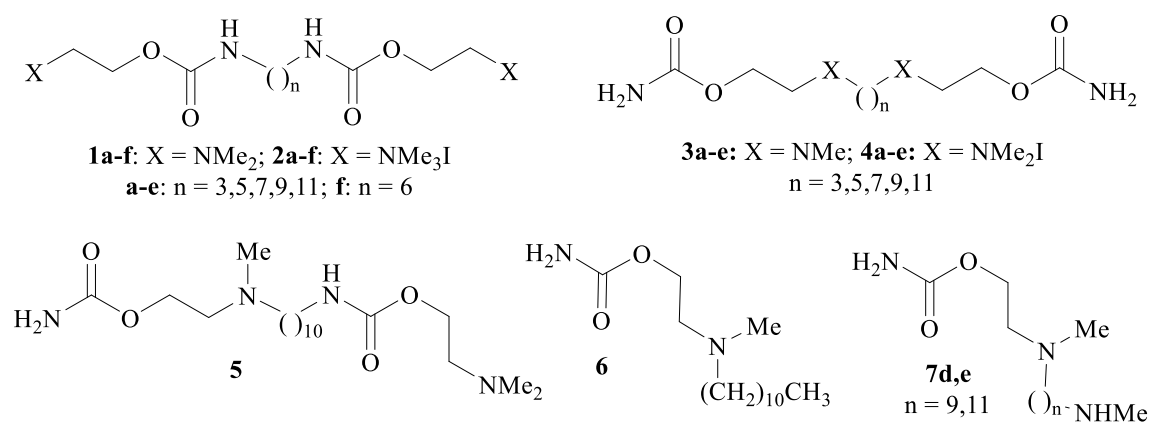
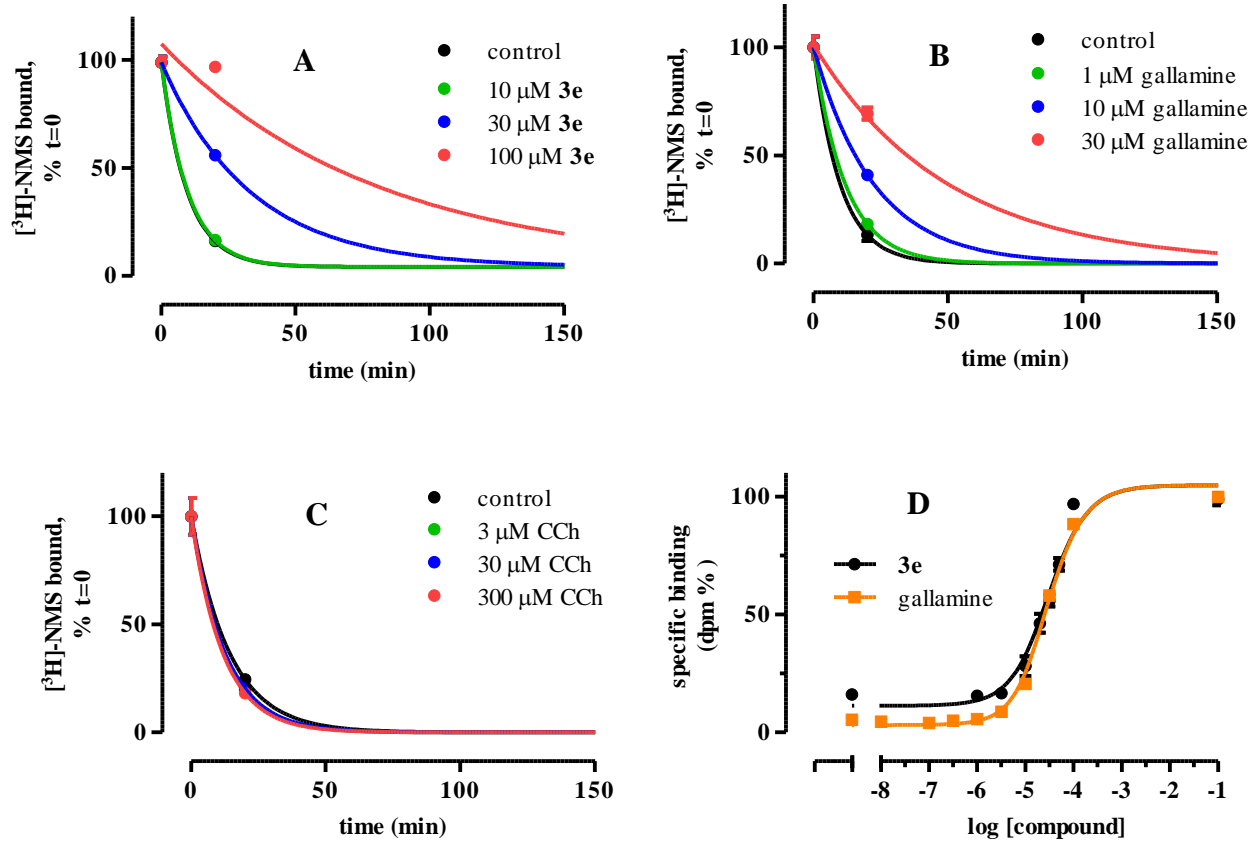


Figure 1

Figure 2



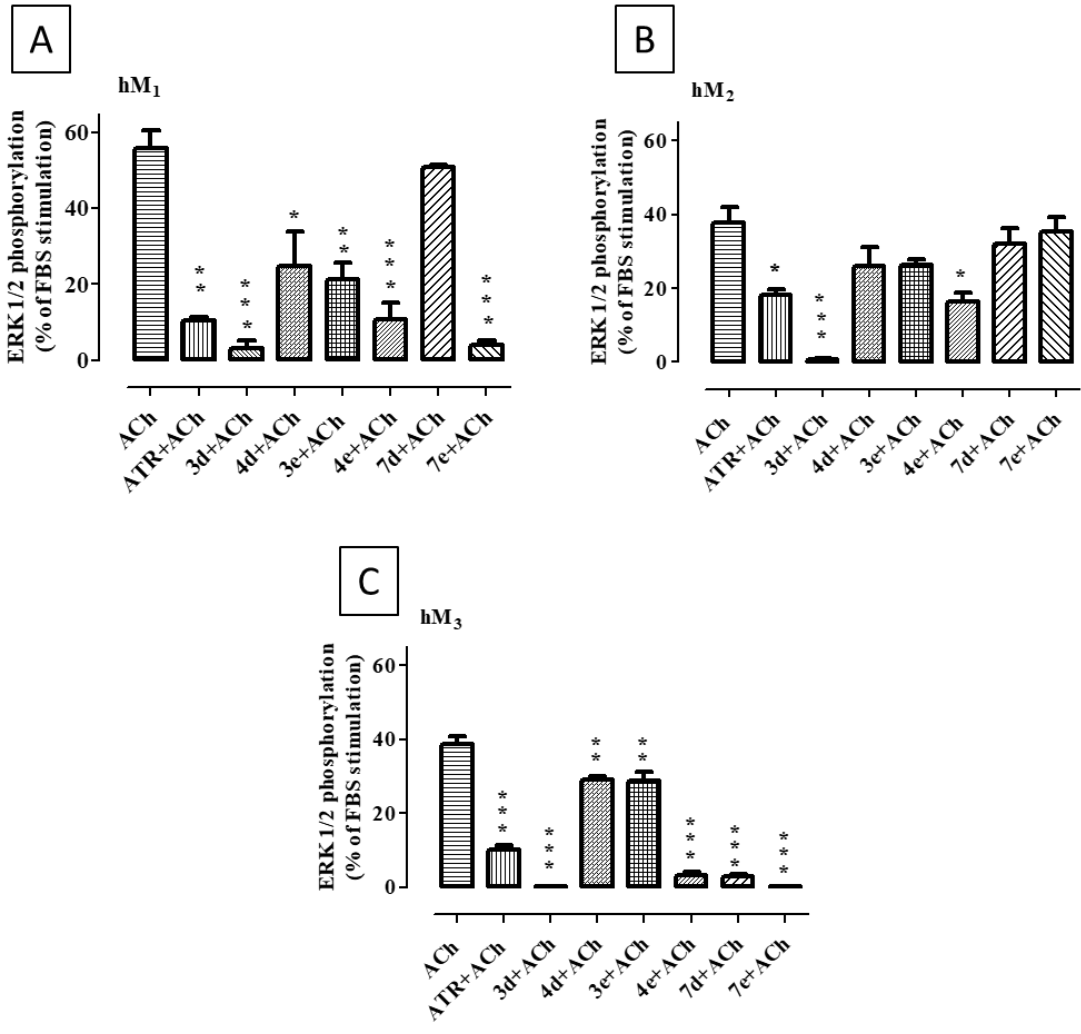


Figure 3

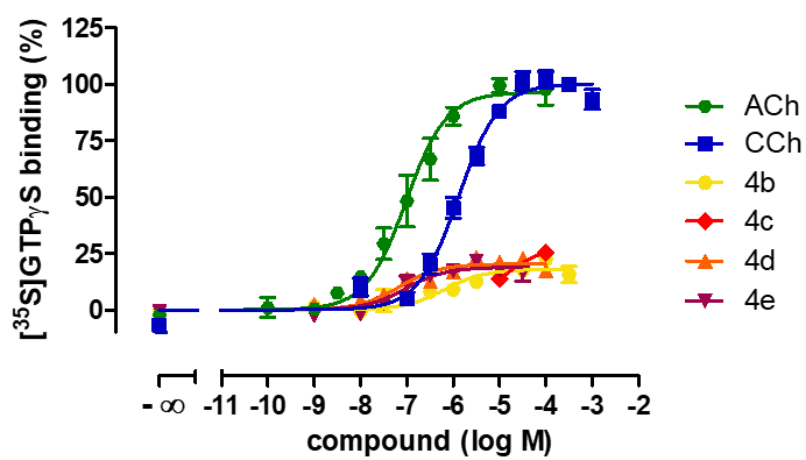


Figure 4

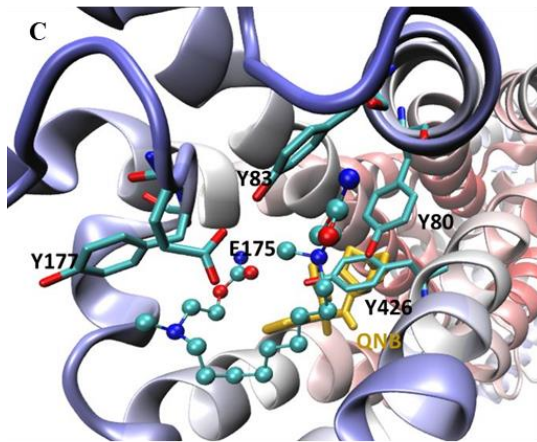
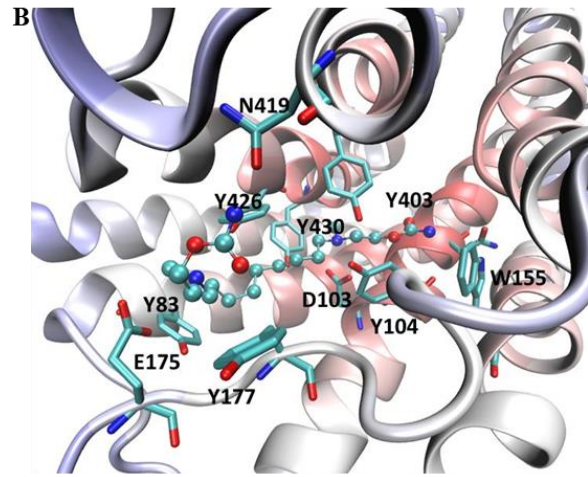
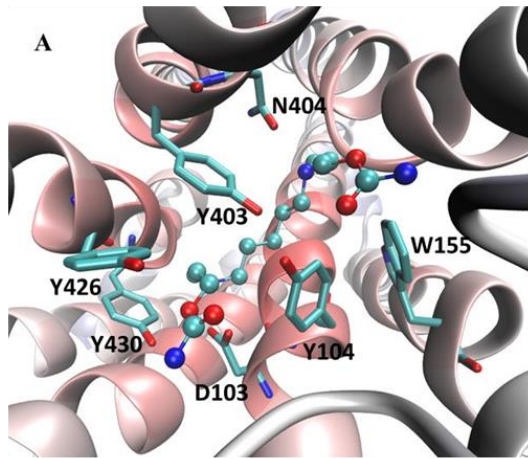


Figure 5